

Menthone Exerts its Antimicrobial Activity Against Methicillin Resistant *Staphylococcus aureus* by Affecting Cell Membrane Properties and Lipid Profile

Wenming Zhao^{1,2,*}, Chengwei Yang^{1,*}, Ning Zhang^{3,*}, Yuanyuan Peng³, Ying Ma³, Keru Gu³, Xia Liu³, Xiaohui Liu³, Xijian Liu³, Yumin Liu⁴, Songkai Li¹, Linjing Zhao³

¹Department of Spinal Surgery, The 940th Hospital of Joint Logistics Support Force of PLA, Lanzhou, People's Republic of China; ²Department of Orthopedics, Zhangye Second People's Hospital, Zhangye, People's Republic of China; ³College of Chemistry and Chemical Engineering, Shanghai University of Engineering Science, Shanghai, People's Republic of China; ⁴Instrumental Analysis Centre, Shanghai Jiao Tong University, Shanghai, People's Republic of China

*These authors contributed equally to this work

Correspondence: Linjing Zhao, College of Chemistry and Chemical Engineering, Shanghai University of Engineering Science, Shanghai, People's Republic of China, Email ljzhao@sues.edu.cn; Songkai Li, Department of Spinal Surgery, The 940th Hospital of Joint Logistics Support Force of PLA, Lanzhou, People's Republic of China, Email lisongkai@gmail.com

Objective: The characteristic constituents of essential oils from aromatic plants have been widely applied as antimicrobial agents in the last decades. However, their mechanisms of action remain obscure, especially from the metabolic perspective. The aim of the study was to explore the antimicrobial effect and mechanism of menthone, a main component of peppermint oil, against methicillin resistant *Staphylococcus aureus* (MRSA).

Methods: An integrated approach including the microbiology and the high-coverage lipidomics was applied. The changes of membrane properties were studied by the fluorescence and electron microscopical observations. The lipid profile was analyzed by ultra-high performance liquid chromatography coupled with quadruple Exactive mass spectrometry (UHPLC-QE-MS). The lipid-related key targets which were associated with the inhibitory effect of menthone against MRSA, were studied by network analysis and molecular docking.

Results: Menthone exhibited antibacterial activities against MRSA, with minimal inhibitory concentration (MIC) and minimal bactericidal concentration (MBC) of 3,540 and 7,080 µg/mL, respectively. The membrane potential and membrane integrity upon menthone treatment were observed to change strikingly. Further, lipids fingerprinting identified 136 significantly differential lipid species in MRSA cells exposed to menthone at subinhibitory level of 0.1× MIC. These metabolites span 30 important lipid classes belonging to glycerophospholipids, glycolipids, and sphingolipids. Lastly, the correlations of these altered lipids, as well as the potential metabolic pathways and targets associated with menthone treatment were deciphered preliminarily.

Conclusion: Menthone had potent antibacterial effect on MRSA, and the mechanism of action involved the alteration of membrane structural components and corresponding properties. The interactions of identified key lipid species and their biological functions need to be further determined and verified, for the development of novel antimicrobial strategies against MRSA.

Keywords: menthone, MRSA, antimicrobial activity, cell membrane, lipid homeostasis, microbial lipidomics, UHPLC-QE-MS

Introduction

Staphylococcus aureus is a common pathogenic microorganism that involved in a variety of clinical infectious diseases including bone and joint infections, skin and soft tissue infections, urinary tract infections, bacteremia, infective endocarditis, and lethal pneumonia.^{1,2} For example, historically, hip fracture patients had high rates of *Staphylococcus aureus* colonization and surgical site infection.³ Previous literature also anticipated that, between 2005 and 2030, total hip

and total knee revisions will increase by 137 and 601%, respectively, with 25% attributed to infection.⁴ In the last decades, due to the abuse of antibiotics, the infection rate of methicillin resistant *Staphylococcus aureus* (MRSA) has increased worldwide, resulting in the increasing risk of mortality, as well as long and expensive hospitalizations.⁵ World Health Organization (WHO) categorized MRSA as high priority human pathogen in the global priority list of multidrug resistant bacteria.^{6,7} Therefore, the development of novel antimicrobial agents for the management of MRSA infection has been urgent and constant.

Essential oils from aromatic plants and their characteristic components have been widely studied and used as antimicrobial agents in the last decades.^{8–10} A previous study reported that the essential oil from peppermint (*Mentha piperita* L.) was the most potent antimicrobial agent against MRSA compared with a variety of other essential oils tested.¹¹ Peppermint oil could also significantly inhibit the formation of biofilm, and inactivate mature biofilm formed by *S. aureus*.¹² Menthone, chemically named 5-methyl-2-(1-methylethyl) cyclohexanone, is one of the most dominant constituents found in peppermint oil. Various biological properties of menthone have become evident, such as antibacterial, antifungal, antibiofilm, and anti-inflammatory activities.¹³ The antibacterial ability of menthone alone and in combination with antibiotics against MRSA strains has been revealed.^{14–16} However, its underlying mechanism of action remains obscure, especially from the metabolic perspective.

Lipids are essential metabolites that have many crucial cellular functions including as membrane structural components, energy and heat sources, signaling molecules, protein recruitment platforms and substrates for posttranslational protein–lipid modification.¹⁷ The lipid homeostasis of biological membranes plays a dominant role for cell viability. Lipid–lipid interactions in bilayer membranes determine the barrier and permeability properties of the membrane.¹⁸ Despite the central role of membrane lipids composition in cellular function, few is known about the precise mechanism that regulate membrane composition.¹⁹ Lipidomics, that was first appeared in 2003 as a subfield of metabolomics, is a powerful tool to study the metabolism of the cellular lipidome.^{20,21} The aim of the study was to explore the in vitro antimicrobial effect and possible mechanism of action of menthone against MRSA. An integrated approach including the traditional microbiology, fluorescence, and electron microscopical observations, as well as determination of membrane lipid composition by a high-coverage lipidomics based on ultra-high performance liquid chromatography coupled with quadruple Exactive mass spectrometry (UPLC-QE-MS) were applied, and the key targets were studied by network analysis and molecular docking.

Material and Methods

Stains and Growth Condition

An experimental strain of *S. aureus* ATCC 43300 was purchased from Institute of industrial microbiology (Shanghai, China), and cultured at 37°C in nutrient broth (NB) medium consisting of 1% peptone, 0.5% NaCl, 0.3% beef extract powder and 1.5% agar, and maintained at 4°C for short-term storage.

Chemicals

Menthone (CAS no. 10458-14-7, >98%) was purchased from Aladdin (Shanghai, China). Methyltert-butyl ether (MTBE), HPLC-grade formic acid and ammonium formate were purchased from Sigma-Aldrich (Saint Louis, MO, USA). MS-grade methanol, acetonitrile and isopropanol were purchased from Fisher Scientific (Chicago, IL, USA). Ultrapure water was freshly prepared by a Milli-Q reference system (Millipore, Bedford, MA, USA). Lipid standards were obtained from Avanti Polar Lipids (Alabaster, AL, USA).

Antibacterial Activity of Menthone

Antibacterial activity of menthone against MRSA was tested using standard Kirby–Bauer disk diffusion according to the guidelines of the Clinical Laboratory Standards Institute (CLSI).²² When MRSA strain was cultivated to the logarithmic growth stage, the culture concentration was diluted to 10⁸ colony forming unit per milliliter (CFU/mL). Subsequently, 60 µL bacterial suspension was inoculated on agar plates. The filter paper containing 10 µL of pure menthone was placed on the surface of the culture dish. The plates were then incubated at 37°C for 16–20 h. Diameters of the inhibitory zone (DIZ) were measured to determine the antimicrobial activity.

Determination of Minimum Inhibitory Concentrations (MIC) and Minimum Bactericidal Concentrations (MBC)

The MIC and MBC of menthone were determined with the standard broth dilution method (CLSI M07-A8). The bacterial suspension was adjusted to an equivalent of 0.5 McFarland standard and then diluted 100 times. Menthone was diluted with NB medium to obtain various concentration ranges of 0.25–8 $\mu\text{L}/\text{m}$ via the twofold dilution method for MIC tests. The bacterial suspension with 0.1% dimethyl sulphoxide was regarded as negative control. The lowest concentration of drug that inhibited the growth of visible bacteria was deemed as MIC. As for MBC, 10 μL of the suspension with a concentration higher than or equal to MIC was spotted on the NB medium and incubated for 16–20 h. The lowest concentration where no bacterial colonies grew on the plate was defined as MBC. The experiment was repeated three times.

Effect of the Menthone on the Growth Curve

The growth curve protocol was used to investigate the bactericidal effects of the menthone. MRSA were inoculated into fresh NB medium overnight and then diluted with the NB medium to the starting inoculum with an $\text{OD}_{600}=0.03$. Menthone was added to the MRSA suspension so that the final concentration was $0.1\times\text{MIC}$. Bacteria treated without menthone was used as a control.

Then the bacteria were cultivated at 37°C with shaking 120 rpm for 0, 2, 4, 6, 10, and 16 h, respectively. At selected time intervals, the OD_{600} values was measured by an ultraviolet spectrophotometer. The experiment was repeated three times.

Membrane Depolarization Assay

The effect of menthone on membrane potential were determined by using a membrane potential sensitive fluorescent probe cyanine dye diSC₃₋₅,^{23,24} which distributes between cells and the medium depending on the cell membrane potential gradient. Briefly, MRSA was cultivated at 37°C overnight, then cells from log phase culture ($\text{OD}_{600} \sim 0.6$, $\sim 2\times 10^8$ CFU/mL) were harvested, washed, and resuspended in 5 mM HEPES buffer at pH 7.2 containing 5 mM glucose and 100 mM potassium chloride. The resuspended MRSA was incubated with diSC₃₋₅ at 0.4 μM for 2 h, and then the fluorescent-labeled MRSA cells were treated with menthone at $0.1\times$, $0.5\times$, $1\times$, or $2\times$ MIC concentrations. Cells suspension without exposure to menthone were used as control. A spectrophotometer (FS-5, Edinburgh, UK) with an excitation wavelength of 622 nm and an emission wavelength of 670 nm was used to detect the fluorescence level.

Scanning Electron Microscopy (SEM)

The effects of the exposure to different concentrations of menthone on the cellular morphology of MRSA were studied by SEM using our previous method.²⁵ Briefly, MRSA cells were grown to the early exponential phase in NB ($\text{OD}_{600} \sim 0.6$), and treated with menthone (at $0.1\times$, $0.5\times$ or $1\times$ MIC concentrations) for 2 h at 37°C , respectively. Then, the suspensions were washed with PBS and centrifuged at 1,000 g for 10 min at 4°C , and pelleted cells were fixed in 2.5% glutaraldehyde overnight at 4°C . The fixed cells were dehydrated in a graded ethanol series, and observed through SEM (Hitachi S-4800, Tokyo, Japan) at a 10 kV accelerating voltage. The cells without exposure to menthone were similarly processed and used as a control.

Transmission Electron Microscopy (TEM)

TEM analysis were performed by previous published method with some modification.²⁶ Briefly, MRSA cells were grown to $\text{OD}_{600} \sim 0.6$, and treated with different concentrations of menthone for 2 h at 37°C . The suspensions were washed with PBS and centrifuged. After fixed with 2.5% glutaraldehyde overnight, the cells were washed with PBS, and post-fixed with osmium tetroxide for 1 h at RT. Then, washed with PBS, and dehydrated with a graded series of ethanol-acetone series. Cells were infiltrated in resin, embedded and left to polymerize for 48 h at 60°C . The ultrathin sections were prepared by ultramicrotome (Leica EM UC7, Germany) and observed through 120 kV TEM (Talos L120C G2, USA).

UHPLC-QE-MS Lipid Fingerprinting

Cell Culture and Quenching

The MRSA strain was cultured with shaking at 120 rpm overnight at 37 °C and then diluted with the NB medium to the starting inoculum with an $OD_{600} \sim 0.03$. Menthone at $0.1 \times MIC$ concentration in dimethyl sulphoxide was added to the MRSA suspension. The mid-logarithmic growth phase bacterial cells ($OD_{600} \sim 0.8$, $\sim 3 \times 10^8$ CFU/mL) were centrifuged at 1000 g for 10 min at 4°C. The cultural medium was removed. Cells were washed with PBS solution, and then quenched with liquid nitrogen. Six replicates of each group were prepared in menthone-treated and untreated groups.

Sample Preparation

Lipids were extracted using the reported method of methyl-tert-butyl ether (MTBE) with minor modification.²⁷ Cells were homogenized and extracted twice using a biphasic solvent system consisted of 1 mL of MTBE, 300 μ L of cold methanol and 250 μ L of water. After incubation and centrifugation, combined upper phases were collected and dried in a vacuum centrifuge. The residue was reconstituted with 100 μ L of methanol and subjected to analysis. Quality control (QC) samples were self-prepared using the pooled extracting solution.

UHPLC-QE-MS Analysis

Vanquish UHPLC system, consisting of a binary pump, a vacuum degasser, an autosampler and a column oven, and Q Exactive plus Mass spectrometer (Thermo Fisher Scientific, CA, USA) were used for lipid fingerprinting. ACQUITY UPLC BEH C18 column (100 \times 2.1 mm, 1.7 μ m; Waters, USA) was used for the separation of lipids, and the column temperature was set to 55°C. The mobile phase A was composed of 10 mM ammonium formate and 0.1 formic acid in acetonitrile: water (60:40, v/v), and mobile phase B was 10 mM ammonium formate and 0.1 formic acid in isopropanol:acetonitrile (90:10, v/v). The gradient elution was conducted as 95/5 \sim 0/100 in 17 min. Flow rate was 0.4 mL/min. The injection volume was 1 μ L for negative ion mode. Mass spectrometer parameters were set as: scan mode, DDA; full scan range, 150 to 2000 amu; spray voltage of 3.0 kV for negative mode; capillary temperature, 320°C; and s-lens RF level of 50 V.

Data Processing and Statistical Analysis

LipidSearch™ Software Version 4.2 (Thermo Scientific, USA), which contains more than 30 lipid classes and 1,500,000 fragmentations, was used for the identification of lipid species based on accurate mass, fragments in MS/MS. Both mass tolerance for precursor and fragment were set to 5 ppm. The lipid molecules with missing value >50% in the group were deleted. Data were imported into SIMCA-P Version 14.1 (Umetrics, Umea, Sweden) for multivariate pattern-recognition of orthogonal partial least-squares (OPLS) discriminant analysis. Seven-fold cross validation was used to estimate the predictive ability of the fitted model. The robustness of OPLS model was assessed by a permutation test. Discriminant variables were determined by the variable importance in the projection (VIP) value (>1), *p*-value obtained from the two-tailed Student's *t*-test (<0.05), and fold-change value (>1.2 or <0.8). The false discovery rate (FDR) was applied to account for multiple testing using the Benjamini and Hochberg method.²⁸ Pearson's correlation analysis was performed by SPSS 25.0 software package (IBM Corporation, Armonk, NY, USA).

Network Analysis and Molecular Docking

The lipids data were imported into Cytoscape 3.7.1 (<https://cytoscape.org/>), to visualize the associations of lipids and their co-regulating characteristics, and construct the metabolites reaction-enzyme-gene network. The genes associated with the significantly changed lipids in menthone treatment group were considered as the potential targets of menthone. Protein-protein interactive network (PPI) was constructed using STRING database.²⁹ Three-dimensional structures of the target proteins were downloaded from the RCSB PDB (<http://www.rcsb.org/>) and UniProtKB (<https://www.uniprot.org/>) database. Molecular docking was performed by AutoDockTools-1.5.6 software. The binding mode of targets and menthone were visualized by PyMOL.

Results

Antibacterial Activity of Menthone Against MRSA

Our results indicated that menthone had antimicrobial activity against MRSA, showing that the DIZ was 11.9 mm, and the MIC and MBC values were 3,540 and 7,080 $\mu\text{g/ml}$, respectively. The growth curves of MRSA treated with menthone were shown in [Supplementary Figure S1](#). Compared with the control group, MRSA showed different growth speeds after treatment with menthone at the concentration of $0.1\times$ MIC.

Effect of Menthone on Alteration of Membrane Potential

Effect of menthone treatment on membrane potential of MRSA cells was evaluated by fluorescent probe diSC₃-5. diSC₃-5 possesses a long lipophilic hydrocarbon chain that can stably bind to lipid molecules on the cell membrane.³⁰ diSC₃-5 can accumulate inside MRSA, and self-fluorescence quenching occurs due to aggregation, resulting in a low fluorescence intensity.²⁴ When the membrane potential changes, diSC₃-5 is redistributed to a new balance causing the fluorescence shift. As shown in [Figure 1](#), the fluorescence levels of MRSA treated with different concentrations of menthone enhanced rapidly, compared with the solvent control. And an obvious dose-effect relationship was observed within the concentration of 0.1 MIC to 2 MIC. Menthone exhibited no fluorescence disturbance of the probe signal (data not shown).

SEM and TEM Observations

Membrane damage caused by menthone was visualized by SEM. As depicted in [Figure 2](#), MRSA cells without menthone treatment possessed a regular and smooth surface ([Figure 2A](#)), whereas the obvious damages were observed upon menthone, including irregularly wrinkled and shriveled in outer surfaces ($0.1\times$ MIC, [Figure 2B](#)), central umbilication and even lysed ($0.5\times$ or $1\times$ MIC, [Figure 2C and D](#)). Subsequently, TEM was used to visualize cell morphology of MRSA at high resolution, and provided direct evidence of the membrane effects caused by menthone. Untreated MRSA appeared normal ([Figure 3A](#)), and treated MRSA samples exhibited several changes on outer cell walls and cytoplasmic membranes, including numerous spherical mesosome-like structures, lack of cytoplasm, separation of cytoplasmic membrane from the cell wall, cell deformation, leakage of cytoplasmic content, and cellular debris from lysed cells ([Figure 3B–H](#)).

Lipidomics Analysis

There is accumulating evidence indicating that small changes in membrane lipid composition can change nano-structures and/or structures of the membranes with new properties.³¹ Thus, the lipid fingerprints of MRSA with and without menthone at $0.1\times$ MIC were profiled using an untargeted lipidomics approach. The representative base peak ion chromatograms in menthone-treated MRSA and control groups were presented in [Supplementary Figure S2](#). A total of 510 lipids species were detected and identified

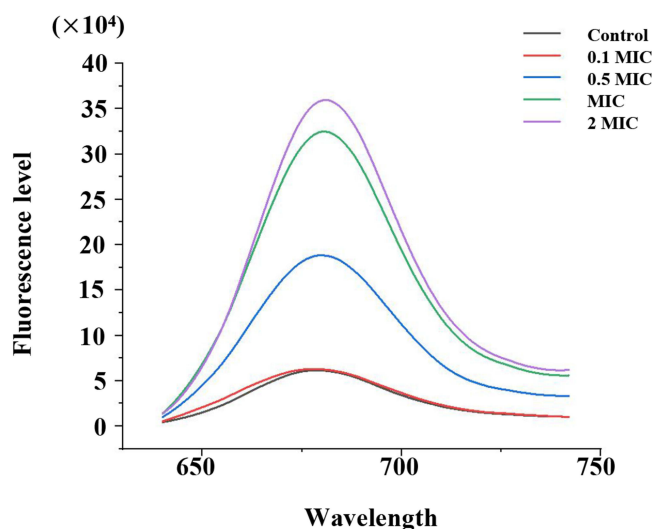


Figure 1 Membrane potential changes upon menthone treatment at concentrations of $0.1\times$, $0.5\times$, $1\times$ and $2\times$ MIC.

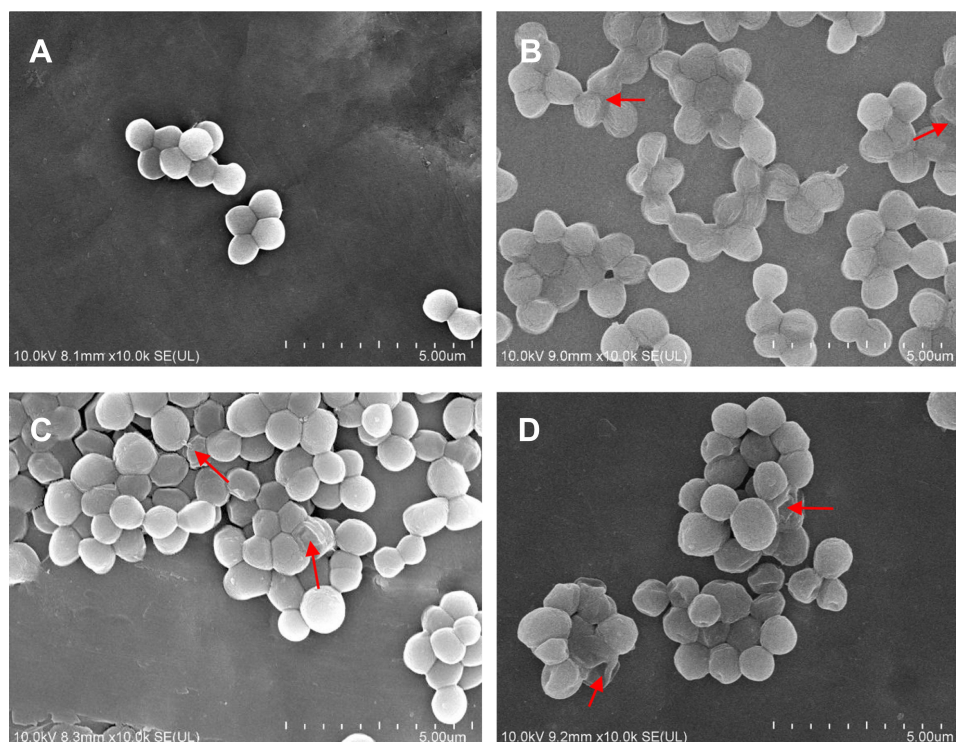


Figure 2 Scanning electron micrographs of untreated MRSA (A) and MRSA treated with menthone at 0.1× MIC (B), 0.5× MIC (C), and 1× MIC (D). The arrows mark areas of membrane damages.

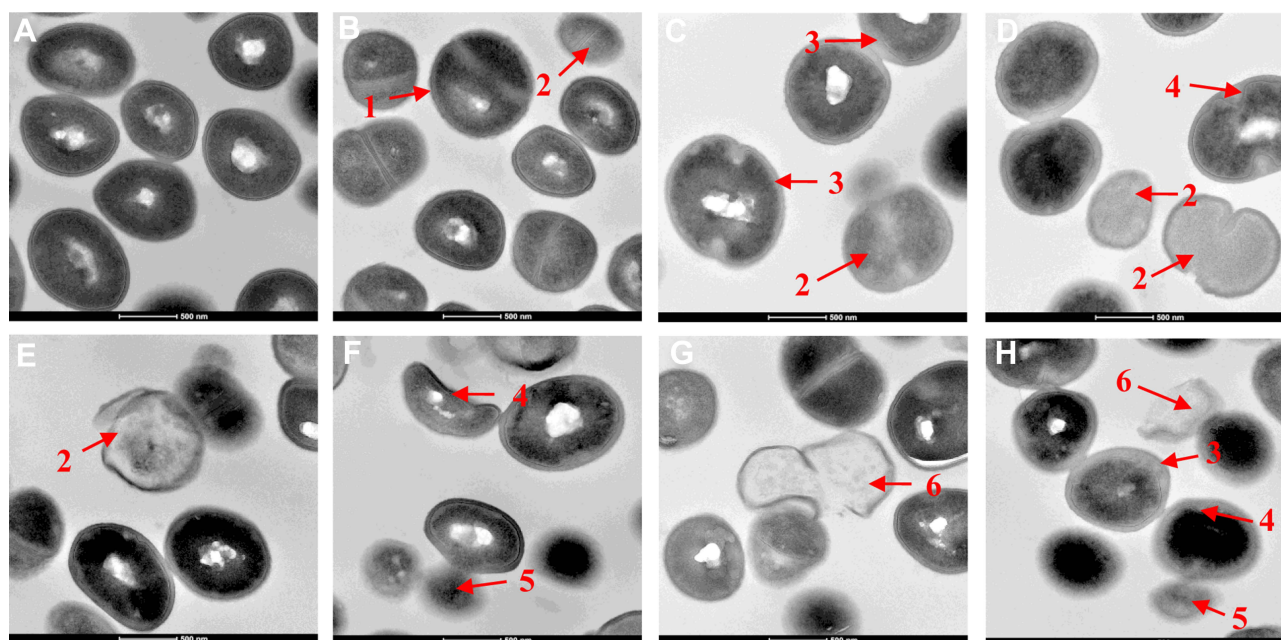


Figure 3 Transmission electron micrographs of untreated MRSA (A) and MRSA treated with menthone at 0.1× MIC (B), 0.5× MIC (C-D), and 1× MIC (E-H). The arrows mark areas of membrane damage and cell content release. 1. numerous spherical mesosome-like structures; 2. lack of cytoplasm; 3. separation of cytoplasmic membrane from the cell wall; 4. cell deformation; 5. leakage of cytoplasmic content; 6. cellular debris from lysed cells.

which present in MRSA cells with and without menthone, with as expected glycerophospholipids, glycolipids, and sphingolipids as the major component. Data quality was assessed by QC samples. Correlation analysis showed good reproducibility between QCs, with the correlation coefficient value of more than 0.99 (Figure 4A). Totally, lipids species that had the relative standard deviation (% RSD) of less than 30%,³² were selected for subsequent statistical analysis.

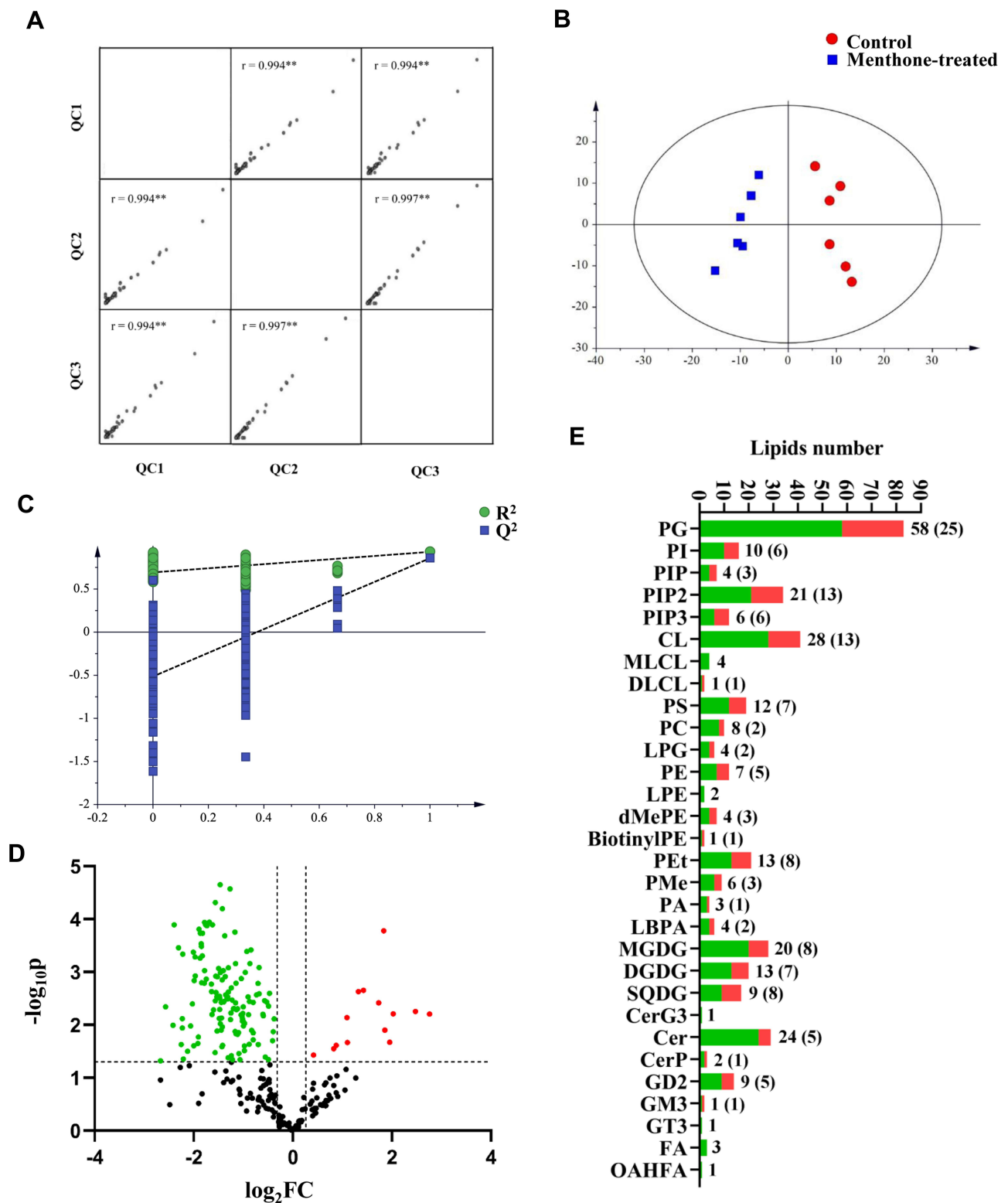


Figure 4 Lipidomic analysis. (A) Data quality control analysis (r , Pearson's correlation coefficient, $**p < 0.01$). (B) Orthogonal partial least squares (O-PLS) graph demonstrating a differential effect of menthone exposure on lipidomic profile of MRSA ($n=6$; $R^2X=0.733$, $R^2Y=0.931$, $Q^2=0.858$). (C) Permutation test result of model (R^2 , explained variance; Q^2 , predictive ability of model). (D) Volcano plot of differential lipid species in menthone-treated group relative to control group. The red and blue dots represent the upregulated and downregulated lipids species, respectively. (E) Quantity of the identified lipid species in each class (green) and significantly differential (red).

The differences of identified lipid classes in MRSA exposed to subinhibitory concentration of menthone were assessed by paired comparison. The percent of the peak intensity of each relative to that of all selected lipid species, which was assigned a value of 100%, was used to establish the relative quantities of lipid classes. The average values were calculated for six biological replicates of each group, menthone-treated and untreated groups. Results indicated that 17 of 30 lipid classes were significantly differential in menthone-treated group relative to controls, as shown in [Supplementary Table S1](#). The levels of phosphatidylcholine (PC), phosphatidic acid (PA), phosphatidylethanol (PEt) and phosphatidylmethanol (PMe), a panel of important membrane components, were significantly elevated in menthone-treated MRSA, whereas the levels of cardiolipin (CL) and its derivative dilysocardiolipin (DLCL), phosphatidylinositol (PI) and other classes (PIP, PIP3), phosphatidylethanolamine (PE) and the derivative glycerophosphoethanolamine-N-biotinyl (BiotinylPE), glycolipids such as digalactosyl diacylglycerol (DGDG) and gangliosides such as GD2 and GD3, were significantly decreased response to menthone. In particular, the altered level of signaling lipid of ceramide (Cer) dramatically elevating ~300% can be observed in menthone group. Besides, the level of nonesterified fatty acid (NEFA) which was potentially associated with the cellular energy storage and metabolism was also increased upon menthone exposure.

To identify the key lipid species response to menthone treatment in MRSA, both multi- and univariate statistical analyses were applied. Multiple pattern recognition of OPLS-DA model for menthone-treated or untreated MRSA, explained 73.3% of X matrix variance (R^2_X) and 93.1% of the discriminant variable (R^2_Y). The fraction of the total variation of X or Y that can be predicted by a component, as estimated by cross validation, was 0.858 (Q^2). As shown in [Figure 4B](#), the samples of MRSA exposed to menthone were well separated with the controls. The permutation test result indicated the robustness of the model ([Figure 4C](#)). The lipid species with higher variable importance in the projection (VIP) scores represent stronger significance of the differences between groups. Further univariate statistical assessment with Student's *t* test and fold change calculation was performed. Volcano plot was used to highlight the differentially expressed lipid species between groups, with *p*-value <0.05 and fold change >1.2 or <0.8 ([Figure 4D](#)). The number of the differential lipid species in each class was shown in [Figure 4E](#). [Table S2](#) showed the significantly differed lipid species between menthone-treated and control groups, including their VIP scores, *p*-values, false discovery rate (FDR), and fold change of their average peak intensity in treatment group versus controls. Totally, 136 significantly altered lipid species were identified, which belong to glycerophospholipids of PG, LPG, PI, PIP, PIP2, PIP3, CL, CLDL, PS, PC, PE, dMePE, biotinylPE, PEt, PMe, PA and LBPA, glycolipids of MGDG, DGDG and SQDG, as well as sphingolipids of Cer, CerP and GD2 and GT3.

The significantly differential lipid species upon menthone treatment cover about 20 lipid classes that participate as bioactive-lipids in multiple signaling pathways of gram-positive bacteria. Therefore, the antimicrobial mechanism underlying the observed difference is complex. Firstly, menthone treatment changes composition of molecular species of glycerophospholipids. The majority of differential lipid species in this study belong to PG, PI, CL, PS, PC, LPG, PE, and PA ([Figure 5](#)), which were important membrane components of *S. aureus*.²⁰ Although the total contents of phosphatidylglycerol (PG) were similar between menthone and control groups, we found the levels of 25 PG species were significantly changed after menthone treatment, most of which were decreased, but four, PG (26:0), PG (33:2), PG (35:2) and PG (38:5+20), were elevated by ~2–4-fold. The levels of all of PI species and their analogs including PIP, PIP2 and PIP3 species were lower upon menthone than that of in controls. Deviations can be observed for CL, in which 12 CL species significantly decreased response to menthone treatment and only one increased, CL (61:0) compared with the controls. Similarly, the levels of 20 PE species and their derivatives of PEt, dMePE and biotinylPE were decreased in the menthone-treated group, whereas the levels of three of PEt, PEt (37:5+4O), PEt (40:8+6O), PEt (42:8+6O), showed a ~2–3-fold increase. The results suggested that menthone may modify the membrane structural components and accordingly change the membrane potential. Furthermore, effect of menthone on another crucial membrane components of glycolipids was observed. A panel of galactolipids significantly decreased including eight monogalactosyldiacylglycerol (MGDG), seven digalactosyldiacylglycerol (DGDG), and eight sulfoquinovosyldiacylglycerol (SQDG) in this study, also suggested menthone may affect the biophysical properties and function of the bilayer ([Figure 6](#)). Secondly, lipids not only served as the major components of membrane, but also the differed lipid classes observed in this study are important precursors of lipoteichoic acid (LTA), suggesting that menthone may disturb the biosynthesis of LTA. LTA are phosphate-

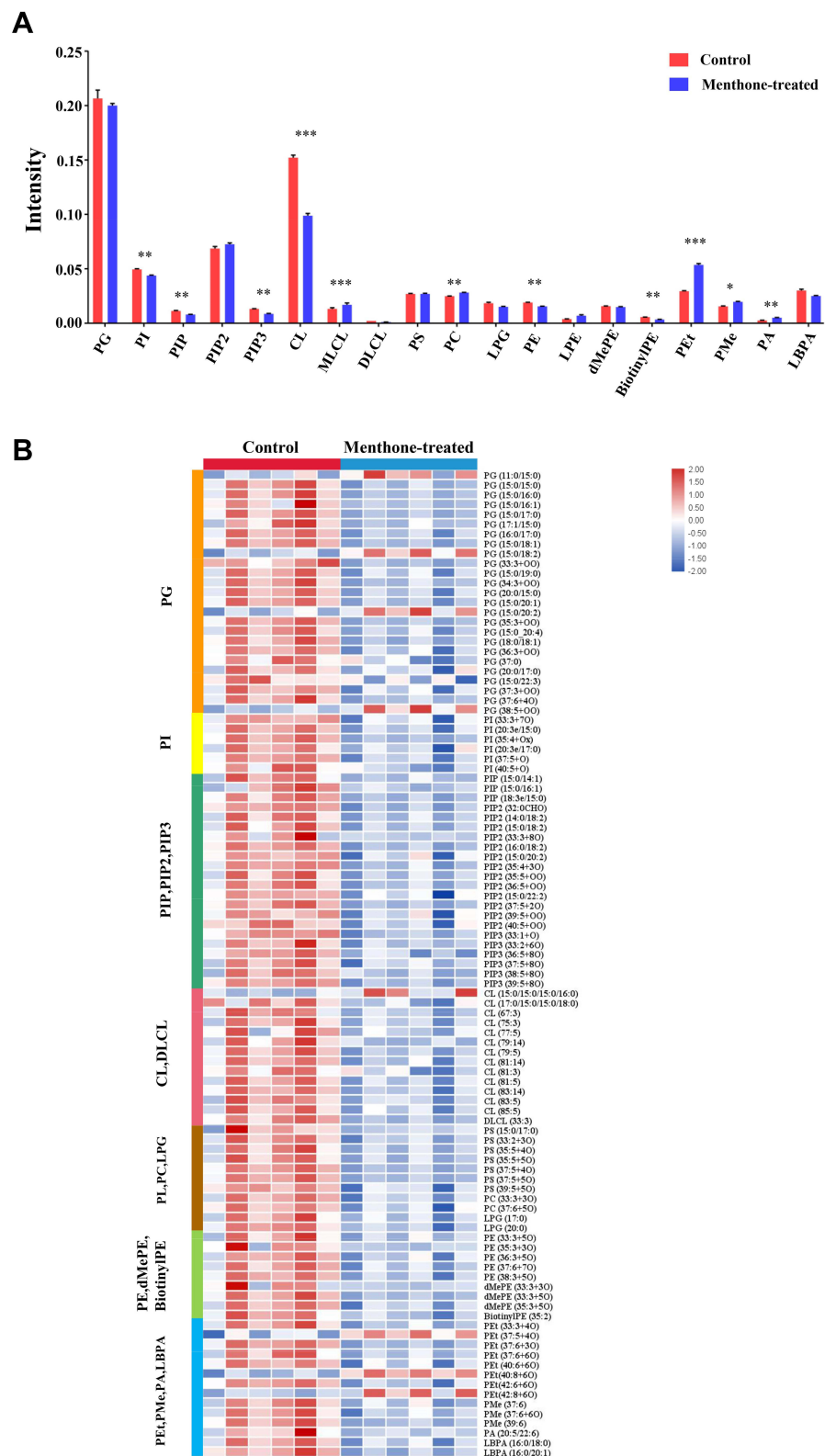


Figure 5 Effect of menthone on glycerophospholipids in MRSA cells. **(A)** The differences of the percentage composition between groups (* $p < 0.05$; ** $p < 0.01$; *** $p < 0.001$). **(B)** Heatmap profiles of glycerophospholipids species in MRSA with and without menthone treatment.

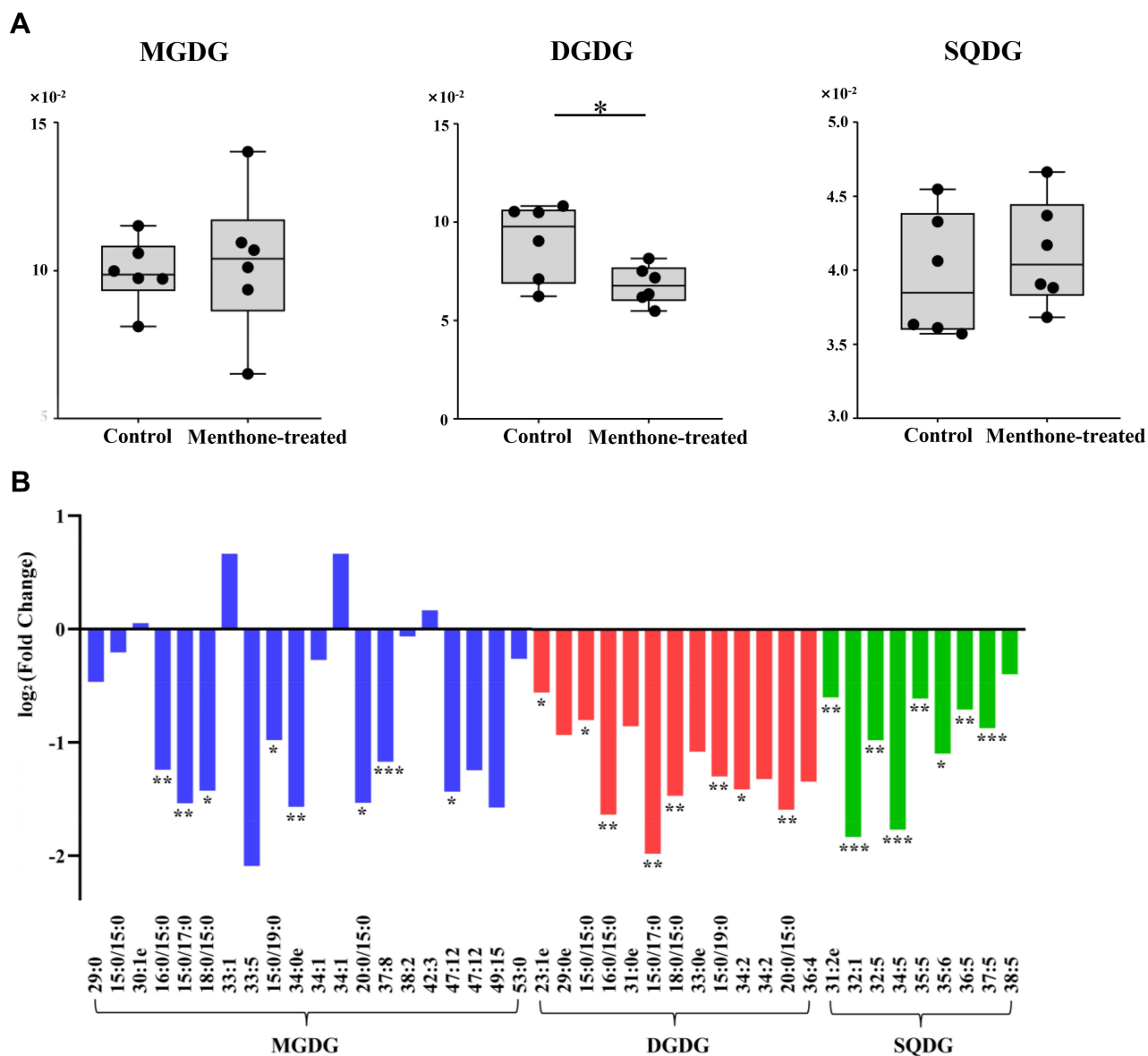


Figure 6 Effect of menthone on glycolipids in MRSA cells. **(A)** The percentage composition of MGDG, DGDG and SQDG in menthone-treated group and control group ($n=6$). **(B)** Fold changes of individual glycolipid species in menthone-treated group compared with controls (* $p<0.05$; ** $p<0.01$; *** $p<0.001$).

containing polymers in the envelope of gram-positive bacteria, which play a dominant role in the growth and physiology of *S. aureus*. The pathway of membrane lipids metabolism and LTA biosynthesis are presented in [Figure 7](#).

Last but remarkably, our lipidome data following menthone treatment showed accumulation of ceramide and reduction of ceramide phosphate (CerP) and gangliosides (such as GD2 and GT3). The latter is a major subtype of sphingolipids composed of ceramide and an oligosaccharide that contains at least one sialic acid residue. The percentage composition of total ceramide elevated ~3-fold upon menthone treatment, and five individual Cer species were found to significantly increase as shown in [Figure 8](#). For example, menthone induced a ~6-fold accumulation of Cer (t42:0+O) and Cer (t43:0+O) in MRSA cells. Meanwhile, the significant decrease levels of seven ceramide derivatives were found after menthone treatment, such as CerP (d39:1+O) (FC=0.615), GD2 d39:1 (FC=0.296) and GT3 d36:2 (FC=0.169), as shown in [Supplementary Table S2](#).

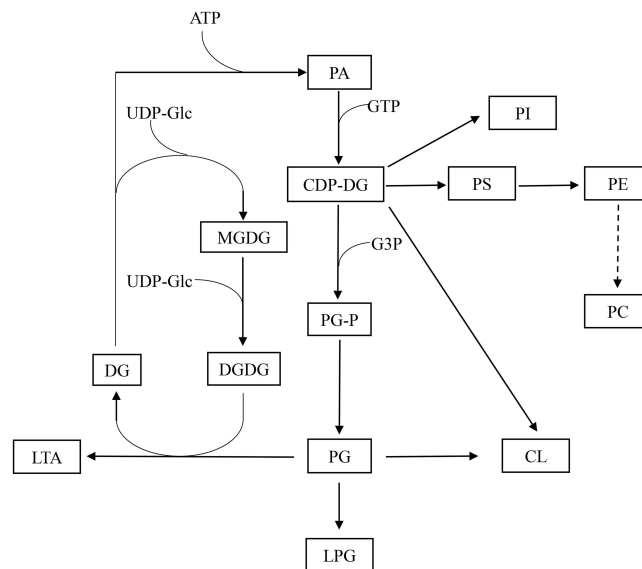


Figure 7 Membrane lipid metabolism and lipoteichoic acid (LTA) biosynthesis in growing *S. aureus*. Similar lipid biosynthesis scheme has been designed for *S. aureus* in previous studies.

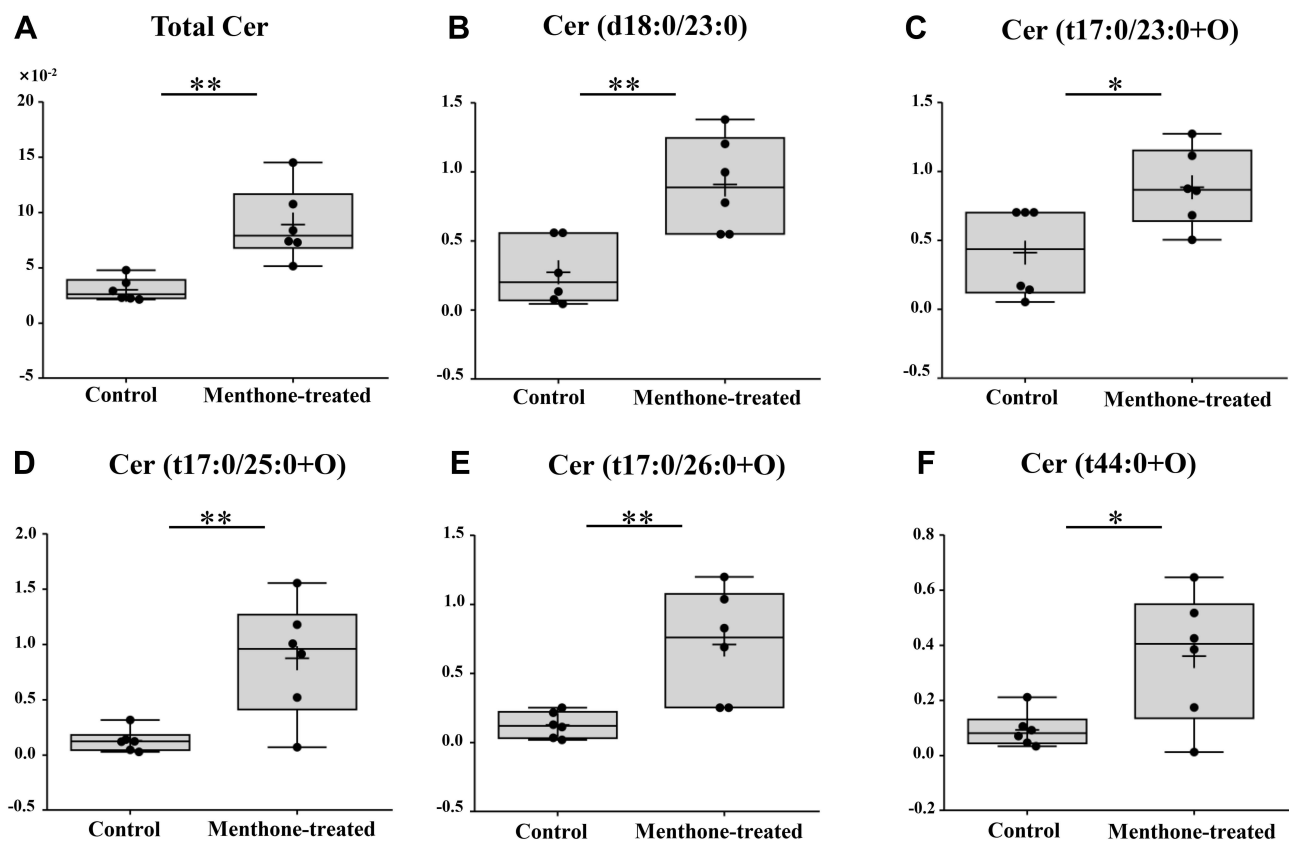


Figure 8 Effect of menthone on ceramides in MRSA cells. Box plots show the differences of percentage composition of total ceramide (A) and the normalized relative intensity of five individual ceramides (B–F). Only the ceramide species that were statistically significant are included in this figure (* $p < 0.05$; ** $p < 0.01$). The entire data set is shown in [Supplementary Table 2](#).

Network Analysis and Molecular Docking

Compositional diversity affects the collective behaviors of lipids in membranes dependent upon lipid-lipid interactions.³³ In this study, metabolic proximities of the discriminatory lipidome were assessed by correlation analysis, to understand the lipid-lipid interaction during the growth inhibition of MRSA. Chord chart visualized the complex associations between both lipid classes and lipid species (Figure 9A). Further, the lipid species with r more than 0.98 ($p < 0.05$) were selected for further network analysis (Figure 9B). There are 88 nodes and 970 edges, which represented the lipid species and their interaction, respectively. The top 15 lipid species with the greatest degree values were PG (15:0/18:1), PI (37:5+O), SQDG (32:1), PEt (37:6+3O), PG (15:0/15:0), PS (37:5+5O), GD2 (d37:1), PG (18:0/18:1), PIP2 (32:0CHO), PIP2 (37:5+2O), PI (35:4+Ox), PG (16:0/17:0), PG (37:6+4O), LBPA (16:0/20:1), and PEt (33:3+4O).

Although it is challenging to understand how lipid compositions are translated into function, totally 85 targets were predicted to possibly associate with the altered lipids profile through metabolites reaction-enzyme-gene database (Figure 10A). And the interactive network of these potential targets was constructed with 80 nodes and 612 edges, as shown in Figure 10B. To validate the main targets responsible for the antimicrobial effect of menthone against MESA, molecular docking was carried out for menthone with the top 10 hub genes which had the highest degree values in PPI network, including PLD2, PLD1, CHPT1, LPCAT4, PPAP2C, PPAP2B, AGPAT3, PEMT, AGPAT2, and PISD. As shown in Figure 11, these targets were successfully docked with menthone, with all negative binding energies of less than -5 . The details are listed in [Supplementary Table S3](#).

Discussion

To our knowledge, there is few study to explore the anti-MRSA mechanism of menthone by lipidomics strategy. In this work, we studied the alterations of lipid profile of MRSA cells treated with menthone using UHPLC-QE-MS, combined with the analyses of membrane potential and integrity. A panel of lipids species which were important components of cell membrane, were found to change significantly in MRSA upon menthone exposure, and the related metabolic pathways and potential targets were further deciphered.

Previous studies reported that many essential oils containing menthone and analogs have antibacterial activity against *S. aureus*.^{34–36} For example, the essential oils of *Mentha piperita* L. contained 22.03% of menthone and 33.28% of menthol had antibacterial activity in gram-positive bacteria of *S. aureus*, with MIC of 0.50 $\mu\text{L/mL}$.³⁷ Tunisian *Mentha aquatica* essential oil was found to be active against *S. aureus* ATCC 29213, which could be correlated to its richness in oxygenated monoterpenes such as menthone accounting for 27.69% of total volatile compounds.³⁸ For MRSA strains, previous study reported that they were susceptible to menthol, which also showed synergistic activity in combination with mupirocin.³⁹ A complex essential oil distillate (Olbas®, Tropfen) with the main component of 1.8-cineol, menthol and menthone displayed a high antimicrobial activity against MRSA, and peppermint oil was the most potent of all individual essential oils tested in a time-kill study.¹¹ Moreover, the EO from *Mentha x piperita* with the major constituents of menthone (22.7%) effectively inhibited growth of multidrug-resistant *S. aureus* strains isolated from clinical materials from humans, although the MIC values showed a wide range from 0.39 mg/mL to 3.12 mg/mL.⁴⁰ Our results indicated that the antimicrobial activity of menthone against MRSA were weaker than several common phenolic EO compounds such as hinokitiol, thymol, carvacrol, and menthol,⁴¹ but comparable to 1.8-cineole.⁴²

The antibacterial mechanism of essential oils containing menthone was rarely reported. Li et al reported that peppermint oil decreased the production of *S. aureus* exotoxins by subinhibitory concentrations in a dose-dependent manner.⁴³ In our study, the antibacterial mode of action of monomer menthone against MRSA was explored first. The diSC3-5 assay²³ result indicated the alteration of membrane potential upon menthone treatment, which is following the reports of antimicrobial components against MRSA extracted from plants,^{44,45} as well as the promising candidates such as amphiphilic neamine derivatives.⁴⁶ SEM and TEM analysis showed that the cells experienced different degrees of destruction. Thus, the depolarizing membrane potential and disrupting bacterial membrane integrity suggested that cell membrane might be the target of menthone against MRSA, and this finding was similar to the antibacterial mechanism of plant essential oils reported previously.^{47,48}

An important characteristic of biological components of essential oils is the hydrophobicity, which enable them to partition the lipids of the bacterial cell membrane and disturb the cell structures.⁴⁹

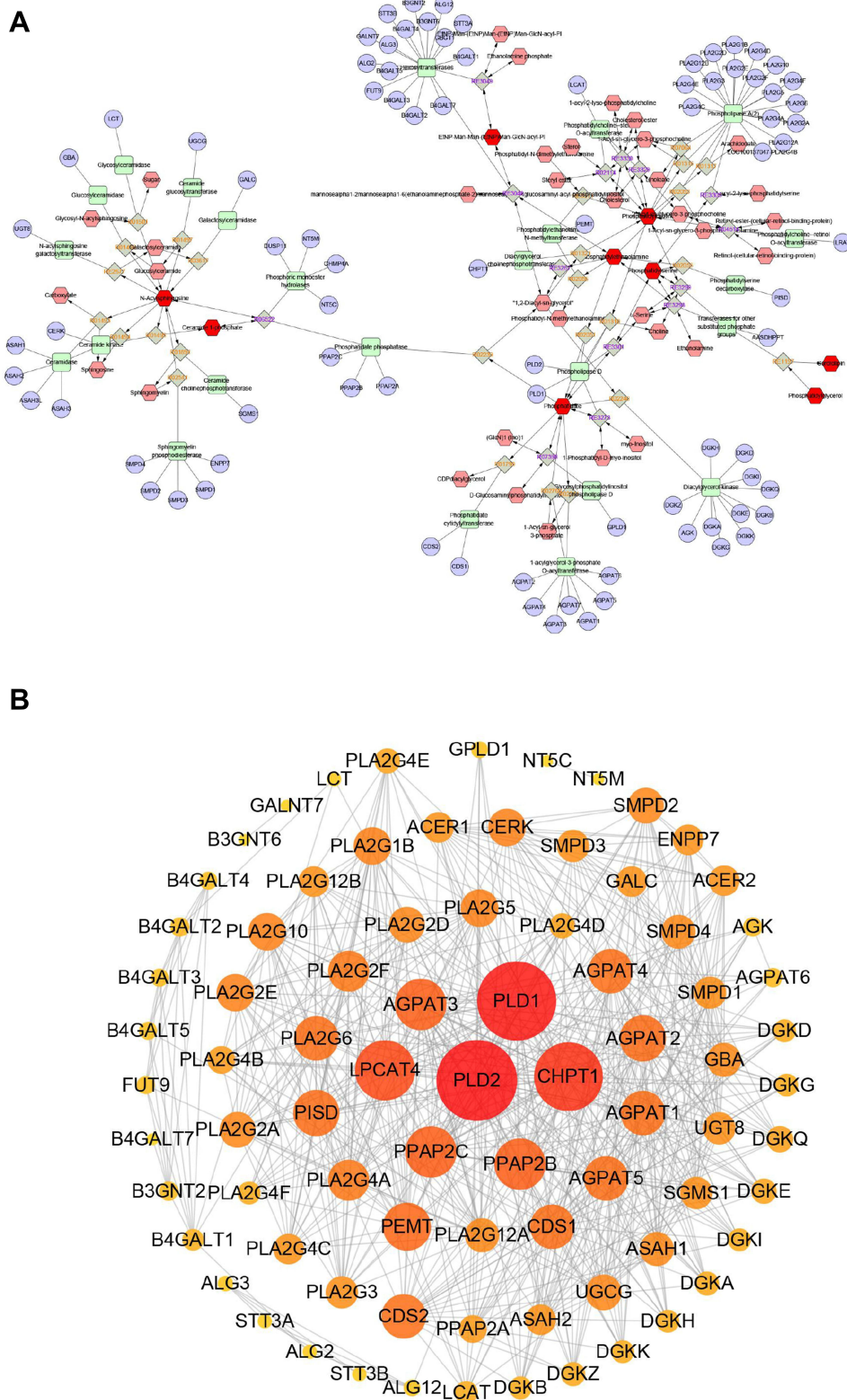


Figure 10 Network analyses results. **(A)** The pathway map of associated lipids-reaction-enzyme gene. The dark red hexagonal represents detected lipids, the shallow red hexagonal represents in-direct metabolites, the green square represents protein, and the blue circle represents genes that coding for the protein. **(B)** The PPIs network by STRING.

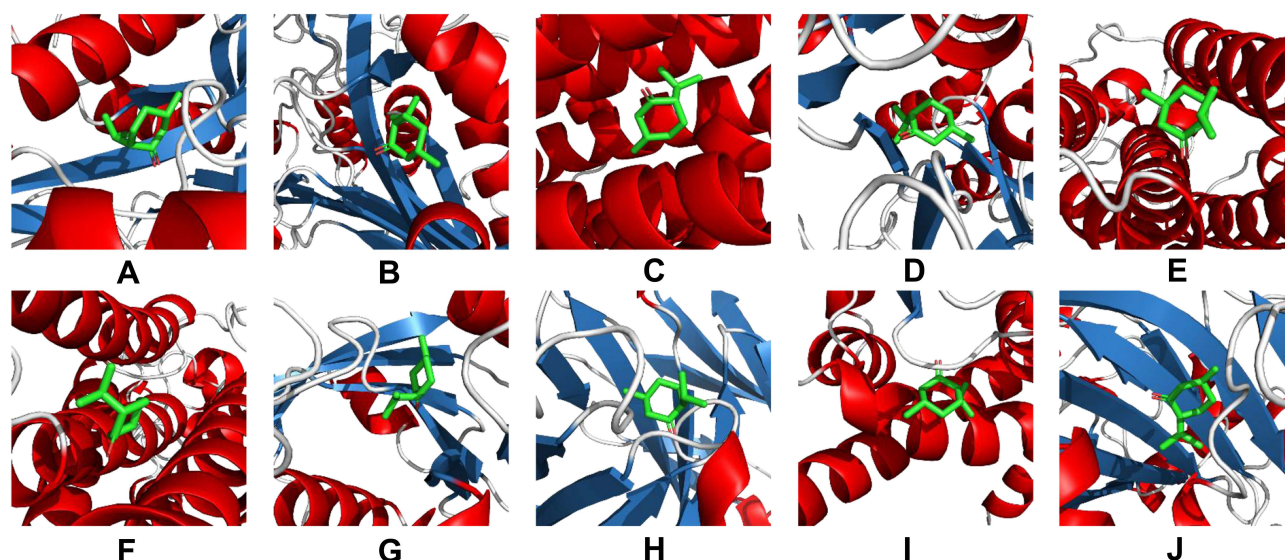


Figure 11 Molecular docking models of menthone binding to the top 10 hub targets of PLD2 (A), PLD1 (B), CHPT1 (C), LPCAT4 (D), PPAP2C (E), PPAP2B (F), AGPAT3 (G), PEMT (H), AGPAT2 (I), and PISD (J). Stick represents menthone; cartoon represents a hub target.

The majority of differential lipid species in this study belong to PG, PI, CL, PS, PC, LPG, PE, and PA, which were important membrane components of prokaryotic cells.^{20,50} The mechanisms of antibacterial activity of a synthetic teixobactin analog Leu₁₀-teixobactin against an MRSA strain were revealed by a profound perturbation in the bacterial membrane lipids.⁵¹ Besides, Pang et al reported that cinnamaldehyde could disrupt cell membrane integrity by moderating the glycerophospholipid biosynthesis pathway of *S. aureus*, especially PG and PE.⁵² Some antimicrobial agents could target CL and play the antibacterial role. Sphingosine could target CL enriched domains, then change cell permeability and lead to cell death.⁵³ Glabrol, a component from licorice flavonoids, displayed strong bactericidal ability. Molecular docking showed that the binding site between glabrol and *S. aureus* was phosphatidylglycerol and CL.⁵⁴ CL could be rapidly synthesized by the regulation of synthase gene *CLS1* under acidic resistance, which improves the survival rate of *S. aureus*.⁵⁵ In addition, our study showed that the levels of glycolipids were significantly changed upon menthone treatment. The association of glycolipid levels with the stability of the membrane has become increasingly evident.⁵⁶

Lipoteichoic acid (LTA) was essential for bacterial growth, which could be a promising target of some antibacterial agents.^{57,58} Yuan et al reported that azalomycin F5a could change the permeability of MRSA and lead to leakage of cellular substances by binding to the polar head of phospholipid and targeting to LTA.⁵⁹ The oxadiazole-containing compound HSGN-94 could inhibit the biosynthesis of LTA in *S. aureus* by binding to PgcA and downregulation of PgsA.^{60,61} Brevibacillin, one of the natural antimicrobial agents, could disrupt cytoplasmic membrane of *S. aureus* by binding to LTA.⁶² Similar lipid biosynthesis scheme has been designed for *S. aureus* in previous studies.^{32,63,64} In general, decreased levels of synthetic precursors of LTA were observed in this study, indicating the biosynthetic disorder of LTA upon menthone.

Sphingolipids, as the important constituents of cell membrane, play an vital role in infection processes, such as the attachment and uptake of pathogenic bacteria.⁶⁵ Ceramide is released from complex sphingolipids, primarily by the activity of sphingomyelinases or is synthesized de novo.⁶⁶ The acid sphingomyelinase-ceramide system plays an important role in the infection of mammalian host cells with *S. aureus*.⁶⁷ The diverse functions of ceramide in bacterial infections have been reported,⁶⁸ such as the induction of apoptosis in infected cells, and regulators of the release of pro-inflammatory cytokines upon infection. Therefore, ceramide and ceramide-enriched membrane domains are thought to potential novel targets to treat infections.⁶⁹

The present study has the strength and limitation. To the best of our knowledge, this is the first evidence to utilize the integrated microbiological and untargeted lipidomic approach to reveal the antimicrobial mechanism of menthone against MRSA. In the premise of good analytical quality control, a large panel of lipid species spanning 30 important lipid classes were focused to study the effect of menthone at subinhibitory concentration on lipid homeostasis of MRSA cells. The key lipid molecules and their interactions that were disturbed upon menthone treatment were considered to associate with the functional

mechanisms of menthone against MRSA. Nevertheless, the effect of menthone on MRSA demands to be consolidated in larger sets of clinical isolates, not only the experimental reference strain. Besides, given that lipid functions are less clear at this moment than the proteins, the combinatory approaches such as lipidomics and proteomics will obtain a better understanding of lipid functions.¹⁷ Interdisciplinary approaches have begun to reveal potential functions of lipids and their interactions recently.⁷⁰

Conclusion

In short, menthone showed potent effect of inhibiting and killing MRSA strain, and the antibacterial mechanism involved the depolarization of membrane potential and disruption of bacterial membrane integrity, as well as the disturbance of lipid homeostasis of MRSA cells. Some targets potentially responsible for the antimicrobial effect were found and validated by network analysis and molecular docking. Our work highlights that lipid fingerprinting could provide a molecular snapshot of complex metabolism of pathogens in response to drug treatment or environmental stress, which might bring innovative solutions to resolve the current challenge.

Abbreviations

PG, phosphatidylglycerol; PI, phosphatidylinositol; PIP, phosphatidylinositol phosphate; PIP₂, phosphatidylinositol diphosphate; PIP₃, phosphatidylinositol triphosphate; CL, cardiolipin; DLCL, dilyscardiolipin; PS, phosphatidylserine; PC, phosphatidylcholine; LPG, lyso phosphatidylcholine; PE, phosphatidylethanolamine; dMePE, dimethylphosphatidylethanolamine; biotinylPE, glycerophosphoethanolamine-N-biotinyl; PEt, phosphatidylethanol; PME, phosphatidylmethanol; PA, phosphatidic acid; MGDG, monogalactosyl diacylglycerol; DGDG, digalactosyl diacylglycerol; SQDG, sulfoquinovosyl diacylglycerol; Cer, ceramide; CerP, ceramide phosphate; GD₂, ganglioside, disialo trihexosyl ceramide; GT₃, ganglioside, trisialo dihexosyl ceramide.

Acknowledgments

This work was funded by the National Natural Science Foundation of China No. 31701032 (to L.Z.).

Disclosure

The authors report no conflicts of interest in this work.

References

1. Brown NM, Goodman AL, Horner C, Jenkins A, Brown EM. Treatment of methicillin resistant *Staphylococcus aureus* (MRSA): updated guidelines from the UK. *JAC Antimicrob Resist*. 2021;3(1):dlaa114. doi:10.1093/jacamr/dlaa114
2. Guo Y, Song G, Sun M, Wang J, Wang Y. Prevalence and therapies of antibiotic- Resistance in *Staphylococcus aureus*. *Front Cell Infect Microbiol*. 2020;10:107. doi:10.3389/fcimb.2020.00107
3. Thyagarajan D, Sunderamoorthy D, Haridas S, Beck S, Praveen P, Johansen A. MRSA colonisation in patients admitted with Hip fracture: implications for prevention of surgical site infection. *Acta Orthop Belg*. 2009;75(2):252–257.
4. Bozic KJ, Kurtz SM, Lau E, Ong K, Vail TP, Berry DJ. The epidemiology of revision total Hip arthroplasty in the United States. *J Bone Joint Surg Am*. 2009;91(1):128–133. doi:10.2106/JBJS.H.00155
5. Grammatico-Guillon L, Baron S, Gettner S, et al. Bone and joint infections in hospitalized patients in France, 2008: clinical and economic outcomes. *J Hosp Infect*. 2012;82(1):40–48. doi:10.1016/j.jhin.2012.04.025
6. Rello J, Kalwaje Eshwara V, Lagunes L, et al. A global priority list of the Top TEN resistant Microorganisms (TOTEM) study at intensive care: a prioritization exercise based on multi-criteria decision analysis. *Eur J Clin Microbiol Infect Dis*. 2019;38(2):319–323. doi:10.1007/s10096-018-3428-y
7. Tacconelli E, Carrara E, Savoldi A, et al. Discovery, research, and development of new antibiotics: the WHO priority list of antibiotic-resistant bacteria and tuberculosis. *Lancet Infect Dis*. 2018;18(3):318–327. doi:10.1016/S1473-3099(17)30753-3
8. Kon KV, Rai MK. Plant essential oils and their constituents in coping with multidrug resistant bacteria. *Expert Rev Anti Infect Ther*. 2012;10(7):775–790. doi:10.1586/eri.12.57
9. Marchese A, Barbieri R, Coppo E, et al. Antimicrobial activity of eugenol and essential oils containing eugenol: a mechanistic viewpoint. *Crit Rev Microbiol*. 2017;43(6):668–689. doi:10.1080/1040841X.2017.1295225
10. Vasconcelos NG, Croda J, Simionatto S. Antibacterial mechanisms of cinnamon and its constituents: a review. *Microb Pathog*. 2018;120:198–203. doi:10.1016/j.micpath.2018.04.036
11. Hamoud R, Sporer F, Reichling J, Wink M. Antimicrobial activity of a traditionally used complex essential oil distillate (Olbas®) Tropfen) in comparison to its individual essential oil ingredients. *Phytomedicine*. 2012;19(11):969–976. doi:10.1016/j.phymed.2012.05.014
12. Kang J, Jin W, Wang J, Sun Y, Wu X, Liu L. Antibacterial and anti-biofilm activities of peppermint essential oil against *Staphylococcus aureus*. *LWT - Food Sci Technol*. 2019;101:639–645. doi:10.1016/j.lwt.2018.11.093

13. Zaia MG, Cagnazzo T, Feitosa KA, et al. Anti-inflammatory properties of menthol and menthone in schistosoma mansoni infection. *Front Pharmacol.* 2016;7:170. doi:10.3389/fphar.2016.00170
14. Kyaw BM, Arora S, Lim CS. Bactericidal antibiotic-phytochemical combinations against methicillin resistant Staphylococcus aureus. *Braz J Microbiol.* 2012;43(3):938–945. doi:10.1590/S1517-83822012000300013
15. Kwiatkowski P, Pruss A, Wojciuk B, et al. The influence of essential oil compounds on antibacterial activity of mupirocin-susceptible and induced low-level mupirocin resistant MRSA strains. *Molecules.* 2019;24(17):17. doi:10.3390/molecules24173105
16. Kwiatkowski P, Lopusiewicz Ł, Pruss A, et al. Antibacterial activity of selected essential oil compounds alone and in combination with β -lactam antibiotics against MRSA strains. *Int J Mol Sci.* 2020;21(19):19. doi:10.3390/ijms21197106
17. Harayama T, Riezman H. Understanding the diversity of membrane lipid composition. *Nat Rev Mol Cell Biol.* 2018;19(5):281–296. doi:10.1038/nrm.2017.138
18. Quinn PJ. Lipid-lipid interactions in bilayer membranes: married couples and casual liaisons. *Prog Lipid Res.* 2012;51(3):179–198. doi:10.1016/j.plipres.2012.01.001
19. de Mendoza D, Pilon M. Control of membrane lipid homeostasis by lipid-bilayer associated sensors: a mechanism conserved from bacteria to humans. *Prog Lipid Res.* 2019;76:100996. doi:10.1016/j.plipres.2019.100996
20. Han X. Lipidomics for studying metabolism. *Nat Rev Endocrinol.* 2016;12(11):668–679. doi:10.1038/nrendo.2016.98
21. Han X, Gross RW. Global analyses of cellular lipidomes directly from crude extracts of biological samples by ESI mass spectrometry: a bridge to lipidomics. *J Lipid Res.* 2003;44(6):1071–1079. doi:10.1194/jlr.R300004-JLR200
22. CLSI. *Performance Standards for Antimicrobial Susceptibility Testing: Twenty-Third Informational Supplement M100-S23.* Wayne, PA, USA: CLSI; 2013.
23. Wu M, Maier E, Benz R, Hancock RE. Mechanism of interaction of different classes of cationic antimicrobial peptides with planar bilayers and with the cytoplasmic membrane of Escherichia coli. *Biochemistry.* 1999;38(22):7235–7242. doi:10.1021/bi9826299
24. Wang B, Pachaiyappan B, Gruber JD, Schmidt MG, Zhang YM, Woster PM. Antibacterial Diamines Targeting Bacterial Membranes. *J Med Chem.* 2016;59(7):3140–3151. doi:10.1021/acs.jmedchem.5b01912
25. Miao Q, Zhao L, Wang Y, et al. Microbial metabolomics and network analysis reveal fungistatic effect of basil (Ocimum basilicum) oil on Candida albicans. *J Ethnopharmacol.* 2020;260:113002. doi:10.1016/j.jep.2020.113002
26. Shen SX, Zhang TH, Yuan Y, Lin SY, Xu JY, Ye HQ. Effects of cinnamaldehyde on Escherichia coli and Staphylococcus aureus membrane. *Food Control.* 2015;47:196–202. doi:10.1016/j.foodcont.2014.07.003
27. Matyash V, Liebisch G, Kurzchalia TV, Shevchenko A, Schwudke D. Lipid extraction by methyl-tert-butyl ether for high-throughput lipidomics. *J Lipid Res.* 2008;49(5):1137–1146. doi:10.1194/jlr.D700041-JLR200
28. Benjamini Y, Hochberg Y. Controlling the false discovery rate: a practical and powerful approach to multiple testing. *J R Stat Soc Series B Stat Methodol.* 1995;57(1):289–300.
29. Szklarczyk D, Franceschini A, Wyder S, et al. STRING v10: protein–protein interaction networks, integrated over the tree of life. *Nucleic Acids Res.* 2015;43(D1):D447D452. doi:10.1093/nar/gku1003
30. Friedrich CL, Moyles D, Beveridge TJ, Hancock RE. Antibacterial action of structurally diverse cationic peptides on gram-positive bacteria. *Antimicrob Agents Chemother.* 2000;44(8):2086–2092. doi:10.1128/AAC.44.8.2086-2092.2000
31. Zhang YM, Rock CO. Membrane lipid homeostasis in bacteria. *Nat Rev Microbiol.* 2008;6(3):222–233. doi:10.1038/nrmicro1839
32. Hewelt-Belka W, Nakonieczna J, Belka M, Bączek T, Namieśnik J, Kot-Wasik A. Untargeted lipidomics reveals differences in the lipid pattern among clinical isolates of staphylococcus aureus resistant and sensitive to antibiotics. *J Proteome Res.* 2016;15(3):914–922. doi:10.1021/acs.jpoteome.5b00915
33. Contreras FX, Ernst AM, Haberkant P, et al. Molecular recognition of a single sphingolipid species by a protein's transmembrane domain. *Nature.* 2012;481(7382):525529. doi:10.1038/nature10742
34. Messaoudi M, Rebiai A, Sawicka B, et al. Effect of extraction methods on polyphenols, flavonoids, mineral elements, and biological activities of essential oil and extracts of Mentha pulegium L. *Molecules.* 2021;27(1):11. doi:10.3390/molecules27010011
35. Reddy DN, Al-Rajab AJ, Sharma M, Moses MM, Reddy GR, Albratty M. Chemical constituents, in vitro antibacterial and antifungal activity of Mentha \times Piperita L. (peppermint) essential oils. *J King Saud Univ Sci.* 2017;31(4):528533.
36. Ghazghazi H, Chedia A, Weslati M, et al. CHEMICAL COMPOSITION AND IN VITRO ANTIMICROBIAL ACTIVITIES OF MENTHA PULEGIUM LEAVES EXTRACTS AGAINST FOODBORNE PATHOGENS. *J Food Saf.* 2013;33(3):239–246. doi:10.1111/jfs.12045
37. Djenane D, Aïder M, Yangüela J, Idir L, Gómez D, Roncalés P. Antioxidant and antibacterial effects of Lavandula and Mentha essential oils in minced beef inoculated with E. coli O157: h7 and S. aureus during storage at abuse refrigeration temperature. *Meat Sci.* 2012;92(4):667–674. doi:10.1016/j.meatsci.2012.06.019
38. Dhifi W, Litaïem M, Jelali N, Hamdi N, Mnif W. Identification of A new chemotype of the plant Mentha aquatica grown in Tunisia: chemical composition, antioxidant and biological activities of its essential oil. *J Essent Oil-Bear Plants.* 2011;14(3):320–328. doi:10.1080/0972060X.2011.10643941
39. Wang F, Liu H, Li J, Zhang W, Jiang B, Xuan H. Australian propolis ethanol extract exerts antibacterial activity against methicillin-resistant Staphylococcus aureus by mechanisms of disrupting cell structure, reversing resistance, and resisting biofilm. *Braz J Microbiol.* 2021;52(4): 1651–1664. doi:10.1007/s42770-021-00547-7
40. Kot B, Wierzchowska K, Piechota M, Czerniewicz P, Chrzanowski G. Antimicrobial activity of five essential oils from Lamiaceae against multidrug-resistant Staphylococcus aureus. *Nat Prod Res.* 2019;33(24):3587–3591. doi:10.1080/14786419.2018.1486314
41. Wang TH, Hsia SM, Wu CH, et al. Evaluation of the antibacterial potential of liquid and vapor phase phenolic essential oil compounds against oral microorganisms. *PLoS One.* 2016;11(9):e0163147. doi:10.1371/journal.pone.0163147
42. Kifer D, Mužinić V, Klarić M. Antimicrobial potency of single and combined mupirocin and monoterpenes, thymol, menthol and 1,8-cineole against Staphylococcus aureus planktonic and biofilm growth. *J Antibiot (Tokyo).* 2016;69(9):689–696.43. doi:10.1038/ja.2016.10
43. Li J, Dong J, Qiu J-Z, Wang, J-F, Li, H-E, Leng, B-F, Ren, W-Z, Deng, X-M. Peppermint oil decreases the production of virulence associated exoproteins by Staphylococcus aureus. *Molecules.* 2011;16(2):1642–1654. doi:10.3390/molecules16021642
44. Wu J, Li B, Xiao W, et al. Longistylin A, a natural stilbene isolated from the leaves of Cajanus cajan, exhibits significant anti-MRSA activity. *Int J Antimicrob Agents.* 2020;55(1):105821. doi:10.1016/j.ijantimicag.2019.10.002

45. Wu SC, Han F, Song MR, et al. Natural flavones from *Morus alba* against methicillin resistant staphylococcus aureus via targeting the proton motive force and membrane permeability. *J Agric Food Chem*. 2019;67(36):10222–10234. doi:10.1021/acs.jafc.9b01795
46. Swain J, El Khoury M, Flament A, et al. Antimicrobial activity of amphiphilic neamine derivatives: understanding the mechanism of action on Gram-positive bacteria. *Biochim Biophys Acta Biomembr*. 2019;1861(10):182998. doi:10.1016/j.bbmem.2019.05.020
47. Marino A, Nostro A, Mandras N, et al. Evaluation of antimicrobial activity of the hydrolate of *Coridothymus capitatus* (L.) Reichenb. fil. (Lamiaceae) alone and in combination with antimicrobial agents. *BMC Complement Med Ther*. 2020;20(1):89. doi:10.1186/s12906-020-2877-x
48. Tang C, Chen J, Zhang L, et al. Exploring the antibacterial mechanism of essential oils by membrane permeability, apoptosis and biofilm formation combination with proteomics analysis against methicillin-resistant staphylococcus aureus. *Int J Med Microbiol*. 2020;310(5):151435. doi:10.1016/j.ijmm.2020.151435
49. Sikkema J, de Bont JA, Poolman B. Interactions of cyclic hydrocarbons with biological membranes. *J Biol Chem*. 1994;269(11):8022–8028. doi:10.1016/S0021-9258(17)37154-5
50. Pinheiro M, Magalhães J, Reis S. Antibiotic interactions using liposomes as model lipid membranes. *Chem Phys Lipids*. 2019;222:36–46. doi:10.1016/j.chemphyslip.2019.05.002
51. Hussein M, Karas JA, Schneider-Futschik EK, et al. The killing mechanism of teixobactin against methicillin resistant staphylococcus aureus: an untargeted metabolomics study. *mSystems*. 2020;5(3):e00077–00020. doi:10.1128/mSystems.00077-20
52. Pang D, Huang Z, Li Q, et al. Antibacterial mechanism of cinnamaldehyde: modulation of biosynthesis of phosphatidylethanolamine and phosphatidylglycerol in staphylococcus aureus and *Escherichia coli*. *J Agric Food Chem*. 2021;69(45):13628–13636. doi:10.1021/acs.jafc.1c04977
53. Verhaegh R, Becker KA, Edwards MJ, Gulbins E. Sphingosine kills bacteria by binding to cardiolipin. *J Biol Chem*. 2020;295(22):7686–7696. doi:10.1074/jbc.RA119.012325
54. Wu S-C, Yang Z-Q, Liu F, et al. Antibacterial effect and mode of action of flavonoids from licorice against methicillin-resistant staphylococcus aureus. *Front Microbiol*. 2019;10. Doi:10.3389/fmicb.2019.02489
55. Ohniwa RL, Kitabayashi K, Morikawa K. Alternative cardiolipin synthase Cls1 compensates for stalled Cls2 function in *Staphylococcus aureus* under conditions of acute acid stress. *Fems microbiology letters*. 2013;338(2):141–146. doi:10.1111/1574-6968.12037
56. Xie J, Bogdanov M, Heacock P, Dowhan W. Phosphatidylethanolamine and monoglucosyldiacylglycerol are interchangeable in supporting topogenesis and function of the polytopic membrane protein lactose permease. *J Biol Chem*. 2006;281(28):19172–19178. doi:10.1074/jbc.M602565200
57. Takagi S, Bai L, Ozeki T, et al. A bovine myeloid antimicrobial peptide (BMAP-28) kills methicillin-resistant *Staphylococcus aureus* but promotes adherence of the bacteria. *Animal Sci J*. 2014;85(3):342–346. doi:10.1111/asj.12109
58. Cao L, Dai C, Li Z, et al. Antibacterial activity and mechanism of a scorpion venom peptide derivative in vitro and in vivo. *PLoS One*. 2012;7(7):e40135. doi:10.1371/journal.pone.0040135
59. Yuan G, Xu L, Xu X, et al. Azalomycin F5a, a polyhydroxy macrolide binding to the polar head of phospholipid and targeting to lipoteichoic acid to kill methicillin-resistant *Staphylococcus aureus*. *Biomed Pharmacother*. 2019;109:1940–1950.
60. Naclerio GA, Abutaleb NS, Onyedibe KI, et al. Mechanistic studies and in vivo efficacy of an oxadiazole containing antibiotic. *J Med Chem*. 2022;65(9):66126630. doi:10.1021/acs.jmedchem.1c02034
61. Sintim HO, Naclerio GA, Karanja CW, Opoku-Temeng C. Antibacterial small molecules that potentially inhibit *Staphylococcus aureus* lipoteichoic acid biosynthesis. *ChemMedChem*. 2019;14(10):1000–1004. doi:10.1002/cmdc.201900053
62. Yang X, Huang E, Yousef AE. Brevibacillin. A cationic lipopeptide that binds to lipoteichoic acid and subsequently disrupts cytoplasmic membrane of *Staphylococcus aureus*. *Microbiol Res*. 2017;195:18–23.
63. Fischer W. Physiology of lipoteichoic acids in bacteria. *Adv Microb Physiol*. 1988;29:233–302.
64. Kuhn S, Slavetinsky CJ, Peschel A. Synthesis and function of phospholipids in *Staphylococcus aureus*. *Int J Med Microbiol*. 2015;305(2):196–202. doi:10.1016/j.ijmm.2014.12.016
65. Kunz TC, Kozjak-Pavlovic V. Diverse facets of sphingolipid involvement in bacterial infections. *Front Cell Dev Biol*. 2019;7. doi:10.3389/fcell.2019.00203
66. Grassmé H, Becker KA. Bacterial infections and ceramide. *Handb Exp Pharmacol*. 2013;216:305–320.
67. Esen M, Schreiner B, Jendrossek V, et al. Mechanisms of *Staphylococcus aureus* induced apoptosis of human endothelial cells. *Apoptosis*. 2001;6(6):431–439. doi:10.1023/A:1012445925628
68. Grassmé H, Jendrossek V, Riehle A, et al. Host defense against *Pseudomonas aeruginosa* requires ceramide-rich membrane rafts. *Nat Med*. 2003;9(3):322–330. doi:10.1038/nm823
69. Grassmé H, Becker KA, Zhang Y, Gulbins E. Ceramide in bacterial infections and cystic fibrosis. *Biol Chem*. 2008;389(11):1371–1379. doi:10.1515/BC.2008.162
70. Pinot M, Vanni S, Pagnotta S, et al. Lipid cell biology. Polyunsaturated phospholipids facilitate membrane deformation and fission by endocytic proteins. *Science*. 2014;345(6197):693–697. doi:10.1126/science.1255288

Drug Design, Development and Therapy

Dovepress

Publish your work in this journal

Drug Design, Development and Therapy is an international, peer-reviewed open-access journal that spans the spectrum of drug design and development through to clinical applications. Clinical outcomes, patient safety, and programs for the development and effective, safe, and sustained use of medicines are a feature of the journal, which has also been accepted for indexing on PubMed Central. The manuscript management system is completely online and includes a very quick and fair peer-review system, which is all easy to use. Visit <http://www.dovepress.com/testimonials.php> to read real quotes from published authors.

Submit your manuscript here: <https://www.dovepress.com/drug-design-development-and-therapy-journal>